

Doping dependence of the redistribution of optical spectral weight in $\text{Bi}_2\text{Sr}_2\text{CaCu}_2\text{O}_{8+\delta}$

F. Carbone, A. B. Kuzmenko, H. J. A. Molegraaf, E. van Heumen, V. Lukovac, F. Marsiglio, and D. van der Marel
Departement de Physique de la Matière Condensée, Université de Genève, 24 Quai Ernest-Ansermet, CH-1211 Geneva 4, Switzerland

K. Haule and G. Kotliar

Department of Physics, Rutgers University, Piscataway, New Jersey 08854, USA

H. Berger and S. Courjault

École Polytechnique Fédérale de Lausanne, Département de Physique, CH-1015 Lausanne, Switzerland

P. H. Kes and M. Li

Kamerlingh Onnes Laboratory, Leiden University, 2300 RA Leiden, The Netherlands

(Received 8 May 2006; revised manuscript received 25 June 2006; published 22 August 2006)

We present the *ab*-plane optical conductivity of four single crystals of $\text{Bi}_2\text{Sr}_2\text{CaCu}_2\text{O}_{8+\delta}$ (Bi2212) with different carrier doping levels from the strongly underdoped to the strongly overdoped range with $T_c=66, 88, 77,$ and 67 K, respectively. We focus on the redistribution of the low frequency optical spectral weight (SW) in the superconducting and normal states. The temperature dependence of the low-frequency spectral weight in the normal state is significantly stronger in the overdoped regime. In agreement with other studies, the superconducting order is marked by an increase of the low frequency SW for low doping, while the SW decreases for the highly overdoped sample. The effect crosses through zero at a doping concentration $\delta=0.19$ which is slightly to the right of the maximum of the superconducting dome. This sign change is not reproduced by the BCS model calculations, assuming the electron-momentum dispersion known from ARPES data. Recent cluster dynamical mean field theory calculations based on the Hubbard and *t*-*J* models, agree in several relevant respects with the experimental data.

DOI: [10.1103/PhysRevB.74.064510](https://doi.org/10.1103/PhysRevB.74.064510)

PACS number(s): 74.25.Gz, 74.25.Jb, 74.72.Hs, 74.20.-z

I. INTRODUCTION

One of the most puzzling phenomena in the field of high temperature superconductivity is the doping dependence of the electronic structure of the cuprates. Several experiments report a conventional Fermi liquid behavior on the overdoped side of the superconducting dome,¹⁻⁴ while the enigmatic pseudogap phase is found in underdoped samples.⁵⁻⁷ In the underdoped and optimally doped regions of the phase diagram it has been shown for bi-layer Bi2212 (Refs. 8–10) and trilayer Bi2223 ($\text{Bi}_2\text{Sr}_2\text{Ca}_2\text{Cu}_3\text{O}_{10}$) (Ref. 11) that the low frequency spectral weight (SW) increases when the system becomes superconducting. This observation points toward a non-BCS-like pairing mechanism, since in a BCS scenario the superconductivity induced SW transfer would have the opposite sign. On the other hand, in Ref. 4 a fingerprint of more conventional behavior has been reported using optical techniques for a strongly overdoped thin film of Bi2212: the SW redistribution at high doping has the opposite sign with respect to the observation for under and optimal doping.

It is possible to relate the SW transfer and the electronic kinetic energy using the expression for the intraband spectral weight SW via the momentum distribution function n_k of the conduction electrons¹²

$$\text{SW}(\Omega_c, T) \equiv \int_0^{\Omega_c} \sigma_1(\omega, T) d\omega = \frac{\pi e^2 a^2}{2\hbar^2 V} \langle -\hat{K} \rangle, \quad (1)$$

where $\sigma_1(\omega, T)$ is the real part of the optical conductivity, Ω_c is a cutoff frequency, a is the in-plane lattice constant, V is the volume of the unit cell, and $\hat{K} \equiv -a^{-2} \sum_k \hat{n}_k \partial^2 \epsilon_k / \partial k^2$. The

operator \hat{K} becomes the exact kinetic energy $\sum_k \hat{n}_k \epsilon_k$ of the free carriers within the nearest-neighbor tight-binding approximation. It has been shown in Refs. 13 and 14, that even after accounting for the next-nearest-neighbor hopping parameter the exact kinetic energy and $\langle -\hat{K} \rangle$ approximately coincide and follow the same trends as a function of temperature. According to Eq. (1), the lowering of $\text{SW}(\Omega_c)$ implies an increase of the electronic kinetic energy and vice versa. In this simple scenario a decrease of the low frequency SW, when the system becomes superconducting, would imply a superconductivity induced increase of the electronic kinetic energy, as it is the case for BCS superconductors.

In the presence of strong electronic correlations this basic picture must be extended to take into account that at different energy scales materials are described by different model Hamiltonians, and different operators to describe the electric current at a given energy scale.^{15,16} In the context of the Hubbard model, Wrobel *et al.* pointed out¹⁷ that if the cutoff frequency Ω_c is set between the value of the exchange interaction $J \approx 0.1$ eV and the hopping parameter $t \approx 0.4$ eV then $\text{SW}(\Omega_c)$ is representative of the kinetic energy of the holes within the *t*-*J* model in the spin polaron approximation and describes the excitations below the on-site Coulomb integral $U \approx 2$ eV not involving double occupancy, while $\text{SW}(\Omega_c > U)$ represents all intraband excitations and therefore describes the kinetic energy of the full Hubbard Hamiltonian. A numerical investigation of the Hubbard model within the dynamical cluster approximation¹⁸ has shown the lowering of the full kinetic energy below T_c , for different doping levels, including the strongly overdoped regime. Experimentally,

this result should be compared to the integrated spectral weight where the cutoff frequency is set well above $U = 2$ eV in order to catch all the transitions into the Hubbard bands. However, in the cuprates this region also contains interband transitions, which would make the comparison rather ambiguous.

Using cluster dynamical mean field theory (CDMFT) on a 2×2 cluster Haule and Kotliar¹⁹ recently found that, while the total kinetic energy decreases below T_c at all doping levels, the kinetic energy of the holes exhibits the opposite behavior on the two sides of the superconducting dome: In the underdoped and optimally doped samples the kinetic energy of the holes, which is the kinetic energy of the t - J model, decreases below T_c . In contrast, on the overdoped side the same quantity increases when the superconducting order is switched on in the calculation. This is in agreement with the observations of Ref. 4 as well as the experimental data in the present paper. The good agreement between experiment and theory in this respect is encouraging, and it suggests that the t - J model captures the essential ingredients, needed to describe the low energy excitations in the cuprates, as well as the phenomenon of superconductivity itself.

The Hubbard model and the t - J model are based on the assumption that strong electron correlations rule the physics of these materials. Based on these models an increase of the low frequency SW in the superconducting state was found in the limit of low doping¹⁷ in agreement with the experimental results.^{8,11} The optical conductivity of the t - J model in a region of intermediate temperatures and doping near the top of the superconducting dome has been recently studied using CDMFT.¹⁹ The CDMFT solution of the t - J model at different doping levels suggests a possible explanation for the fact that the optical spectral weight shows opposite temperature dependence for the underdoped and the overdoped samples. It is useful to think of the kinetic energy operator of the Hubbard model at large U as composed of two physically distinct contributions representing the superexchange energy of the spins and the kinetic energy of the holes. The superexchange energy of the spins is the result of the virtual transitions across the charge transfer gap, thus, the optical spectral weight integrated up to an energy below these excitations is representative only of the kinetic energy of the holes. The latter contribution to the total kinetic energy was found to decrease in the underdoped regime while it increases above optimal doping, as observed experimentally. This kinetic energy lowering is however rather small compared to the lowering of the superexchange energy. Upon overdoping the kinetic energy of the holes increases in the superconducting state, while the larger decrease of the superexchange energy makes superconductivity favorable with a still high value of T_c . In the CDMFT study of the t - J model, a stronger temperature dependence of $SW(T)$ is found on the overdoped side. This reflects the increase in Fermi liquid coherence with reducing temperature.

In the present paper we extend earlier experimental studies of the temperature-dependent optical spectral weight of Bi2212 by the same group^{8,10} to the overdoped side of the phase diagram, i.e., with superconducting phase transition temperatures of 77 K and 67 K. We report a strong change in magnitude of the temperature dependence in the normal state

for the sample with the highest hole doping, and we show that the kink in the temperature dependence at T_c changes sign at a doping level of about 19% (which is the sample where the absolute value of the effect must be smaller than $0.02 \times 10^6 \Omega^{-1} \text{cm}^{-2}$), in qualitative agreement with the report by Deutscher *et al.*⁴

II. EXPERIMENT AND RESULTS

In this paper we concentrate on the properties of single crystals of Bi2212 at four different doping levels, characterized by their superconducting transition temperatures. The preparation and characterization of the underdoped sample (UD66K), an optimally doped crystal (OpD88) and an overdoped sample (OD77) with T_c 's of 66, 88, and 77 K, respectively, have been given in Ref. 8. The crystal with the highest doping level (OD67) has a T_c of 67 K. This sample has been prepared with the self-flux method. The oxygen stoichiometry of the single crystal has been obtained in a PARR autoclave by annealing for 4 days in oxygen at 140 atmospheres and slowly cooling from 400 °C to 100 °C. The infrared optical spectra and the spectral weight analysis of samples UD66 and OpD88 have been published in Refs. 8 and 10. The phase of $\sigma(\omega)$ of sample OD77 has been presented as a function of frequency in a previous paper.²⁰ In the present paper we present the optical conductivity of samples OD77 and OD67 for a dense sampling of temperatures, and we use this information to calculate $SW(\Omega_c, T)$. The samples are large ($4 \times 4 \times 0.2 \text{ mm}^3$) single crystals. The crystals were cleaved within minutes before being inserted into the optical cryostat. We measured the real and imaginary part of the dielectric function with spectroscopic ellipsometry in the frequency range between 6000 and 36 000 cm^{-1} (0.75–4.5 eV). Since the ellipsometric measurement is done at a finite angle of incidence (in our case 74°), the measured pseudodielectric function corresponds to a combination of the ab -plane and c -axis components of the dielectric tensor. From the experimental pseudodielectric function and the c -axis dielectric function of Bi2212 (Ref. 21) we calculated the ab -plane dielectric function. In accordance with earlier results on the cuprates^{11,22} and with the analysis of Aspnes,²³ the resulting ab -plane dielectric function turns out to be very weakly sensitive to the c -axis response and its temperature dependence. In the range from 100 to 7000 cm^{-1} (12.5–870 meV) we measured the normal incidence reflectivity, using gold evaporated *in situ* on the crystal surface as a reference.

The infrared reflectivity is displayed for all the studied doping levels in Fig. 1. The absolute reflectivity increases with increasing doping, as expected since the system becomes more metallic. Interestingly, the curvature of the spectrum also changes from under to overdoping; this is reflected in the frequency dependent scattering rate as has been pointed out recently by Wang *et al.*²⁴ In order to obtain the optical conductivity in the infrared region we used a variational routine that simultaneously fits the reflectivity and ellipsometric data yielding a Kramers-Kronig (KK) consistent dielectric function which reproduces all the fine features of the measured spectra. The details of this approach are described elsewhere.^{11,25} All data were acquired in a mode of

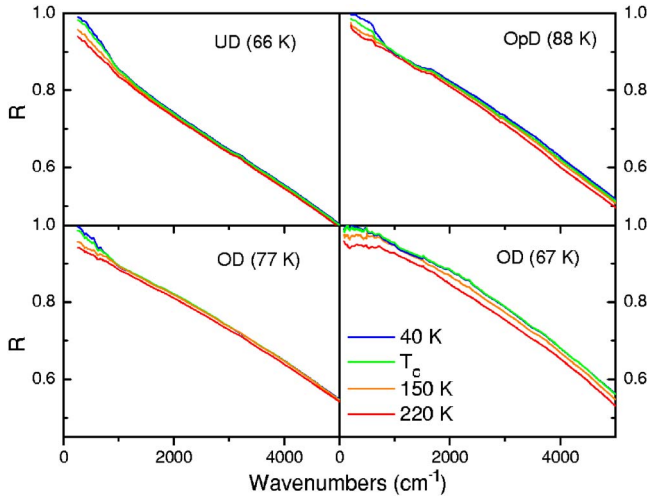


FIG. 1. (Color online) Reflectivity spectra of Bi2212 at selected temperatures for different doping levels, described in the text.

continuous temperature scans between 20 K and 300 K with a resolution of 1 K. Very stable measuring conditions are needed to observe changes in the optical constants smaller than 1%. We use homemade cryostats of a special design, providing a temperature independent and reproducible optical alignment of the samples. To avoid spurious temperature dependencies due to adsorbed gases at the sample surface, we use an ultrahigh vacuum UHV cryostat for the ellipsometry in the visible range, operating at a pressure in the 10^{-10} mbar range, and a high vacuum cryostat for the normal incidence reflectivity measurements in the infrared, operating in the 10^{-7} mbar range.

In Fig. 2 we show the optical conductivity of the two overdoped samples of Bi2212 with $T_c=77$ K and $T_c=67$ K at selected temperatures. Below 700 cm^{-1} one can clearly see the depletion of the optical conductivity in the region of the gap at low temperatures (shown in the inset). The much smaller absolute conductivity changes at higher energies, which are not discernible at this scale, will be considered in detail below.

One can see the effect of superconductivity on the optical constants in the temperature dependent traces, displayed in Fig. 3, at selected energies, for the two overdoped samples. In comparison to the underdoped and optimally doped samples^{8,11} where reflectivity is found to have a further increase in the superconducting state at energies between 0.25 and 0.7 eV, in the overdoped samples the reflectivity decreases below T_c or remains more or less constant. In the strongly overdoped sample one can clearly see, for example, at 1.24 eV, that at low temperature ϵ_1 increases while cooling down, opposite to the observation on the optimally and underdoped samples. These details of the temperature dependence of the optical constants influence the integrated SW trend as we will discuss in the following sections.

III. DISCUSSION

A. Spectral weight analysis of the experimental data

As it is discussed in our previous presentations,^{10,11,25} using the knowledge of both σ_1 and ϵ_1 we can calculate the low

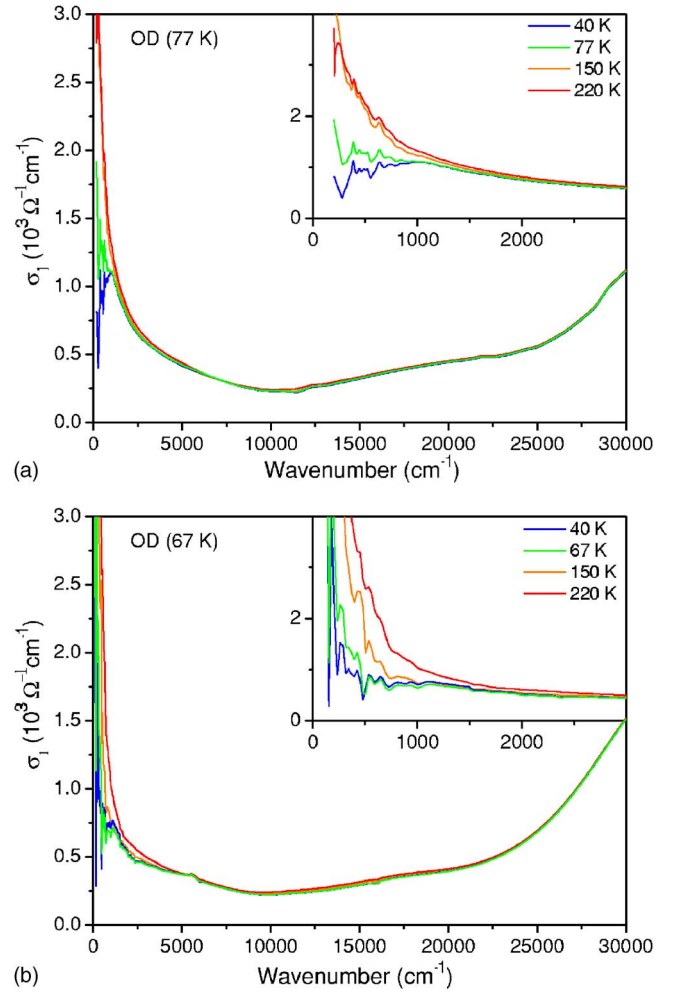


FIG. 2. (Color online) In-plane optical conductivity of slightly overdoped ($T_c=77$ K, top panel) and strongly overdoped ($T_c=67$ K, bottom panel) samples of Bi2212 at selected temperatures. The insets show the low energy parts of the spectra.

frequency SW without the need of the knowledge of σ_1 below the lowest measured frequency. When the upper frequency cutoff of the SW integral is chosen to be lower than the charge transfer energy (around 1.5 eV), the SW is representative of the free carrier kinetic energy in the t - J model.^{11,17,19} In this paper we set the frequency cutoff at 1.25 eV and compare the results with the predictions of BCS theory and CDMFT calculations based on the t - J model. In Fig. 4 we show a comparison between SW(T) for different samples with different doping levels. One can clearly see that the onset of superconductivity induces a positive change of the SW(0–1.25 eV) in the underdoped sample and in the optimally doped one,⁸ in the 77 K sample no superconductivity induced effect is detectable for this frequency cutoff and in the strongly overdoped sample we observe a decrease of the low frequency spectral weight. In the right-hand panel of Fig. 4 we also display the derivative of the integrated SW as a function of temperature. The effect of the superconducting transition is visible in the underdoped sample and in the optimally doped sample as a peak in the derivative plot; no effect is detectable in the overdoped 77 K sample, while in

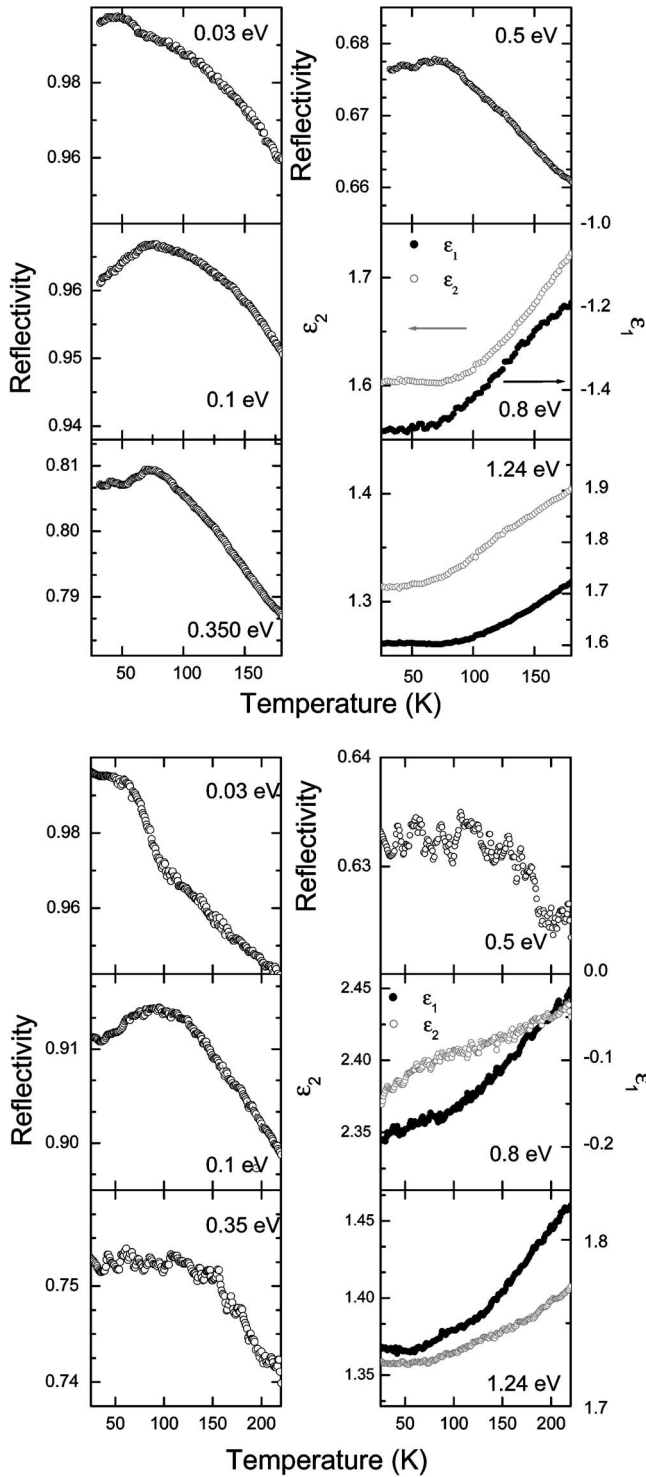


FIG. 3. Topmost (lower) panel: reflectivity and dielectric function of sample OD67 (OD77) as a function of temperature for selected photon energies. The corresponding photon energies are indicated in the panels. The real (imaginary) parts of $\epsilon(\omega)$ are indicated as closed (open) symbols.

the strongly overdoped sample a change in the derivative of the opposite sign is observed.

The frequency ω_p^* for which $\epsilon_1(\omega_p^*)=0$ corresponds to the eigenfrequency of the longitudinal oscillations of the free

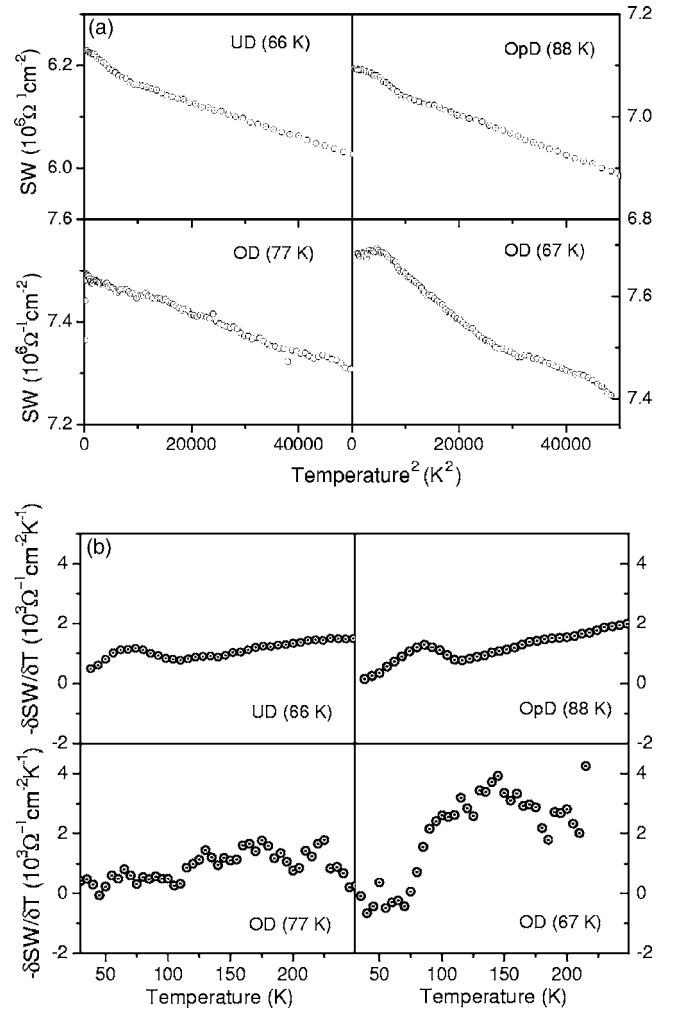


FIG. 4. Top panel, spectral weight $SW(\Omega_c, T)$ for $\Omega_c=1.24$ eV, as a function of temperature for different doping levels. Bottom panel, the derivative $(-\frac{\partial SW(\Omega_c, T)}{\partial T})$ as a function of temperature for different doping levels. For the derivative curves the data have been averaged in 5 K intervals in order to reduce the noise.

electrons for $k \rightarrow 0$. ω_p^* can be read off directly from the ellipsometric spectra, without any data processing. The temperature dependence of ω_p^* is displayed in Fig. 5. The screened plasma frequency has a redshift as temperature increases, due to the bound-charge polarizability, and the inter-band transitions. Therefore its temperature dependence can be caused by a change of the free carrier spectral weight, the dissipation, the bound-charge screening, or a combination of those. This quantity can clarify whether a real superconductivity-induced change of the plasma frequency is already visible in the raw experimental data. In view of the fact that the value of ω_p^* is determined by several factors, and not only the low frequency SW, it is clear that the SW still must be determined from the integral of Eq. (1). It is perhaps interesting and encouraging to note, that in all cases which we have studied up to date, the temperature dependences of $SW(T)$ and $\omega_p^*(T)^2$ turned out to be very similar.

One can clearly see in the underdoped and in the optimally doped sample that superconductivity induces a blue-shift of the screened plasma frequency. In the 77 K sample

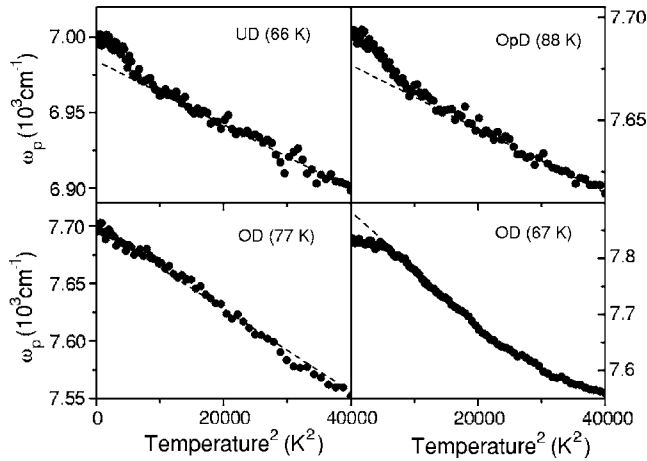


FIG. 5. Screened plasma frequency as a function of temperature for different doping levels.

no effect is visible at T_c while the 67 K sample shows a redshift of the screened plasma frequency. The behavior of the screened plasma frequency also seems to exclude the possibility that a narrowing or a shift with temperature of the interband transitions around 1.5 eV is responsible for the observed changes in the optical constants. If this would be the case then one would expect the screened plasma frequency to exhibit a superconductivity-induced shift in the same direction for all the samples.

B. Predictions for the spectral weight using the BCS model

In order to put the data into a theoretical perspective, we have calculated $SW(T)$ in the BCS model, using a tight-binding parametrization of the energy-momentum dispersion of the normal state. The parameters of the parametrization are taken from ARPES data.²⁶ The details of this calculation are discussed in the Appendix. Because in this parametrization both t' and t'' are taken to be different from zero, the spectral weight is not strictly proportional to the kinetic energy. Nonetheless for the range of doping considered here, SW follows the same trend as the actual kinetic energy, as has been pointed out previously. Results for the t - t' - t'' model are shown in Fig. 6. We do wish to make a cautionary remark here, that a sign change as a function of doping is not excluded *a priori* by the BCS model. However, in the present case this possibility appears to be excluded in view of the state of the art ARPES results for the energy-momentum dispersion of the occupied electron bands. One can see that for all doping levels considered, SW decreases below T_c , thus BCS calculations fail to reproduce the temperature dependence in the underdoped and optimally doped samples. However Norman and Pépin²⁷ first pointed out that a modification of the scattering rate when the material goes superconducting, as seen in ARPES data, naturally leads to the observed SW anomaly in underdoped samples. Furthermore, they found a sign change with increased doping, in qualitative agreement with our observations. Since the modification of the scattering rate presumably models inelastic scattering by electronic degrees of freedom, this description does not nec-

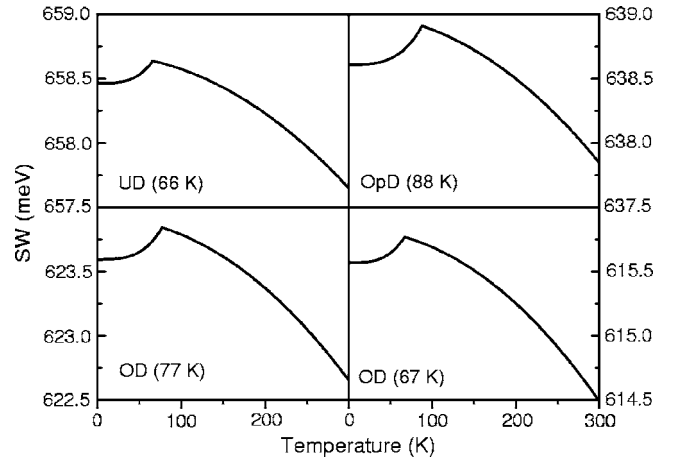


FIG. 6. BCS calculations of the low frequency SW as a function of temperature calculated for the same doping levels experimentally measured.

essarily present a point of view which is orthogonal to the CDMFT calculation which is presented here.

C. Superconductivity induced transfer of spectral weight: experiment and cluster DMFT calculations

In order to highlight the effect of varying the doping concentration, we have extrapolated the temperature dependence in the normal state of $SW(\Omega_c, T)$ of each sample to zero temperature, and measured its departure from the same quantity in the superconducting state, also extrapolated to $T=0$: $\Delta SW_{sc} \equiv SW(T=0) - SW_n^{ext}(T=0)$. In Fig. 7 the experimentally derived quantities are displayed together with the recent CDMFT calculations of the t - J (Ref. 19) model and those based on the BCS model explained in the preceding section. While the BCS-model provides the correct sign only for the strongly overdoped case, the CDMFT calculations based on the t - J model are in qualitative agreement with our data and the data in Ref. 4, insofar both the experimental

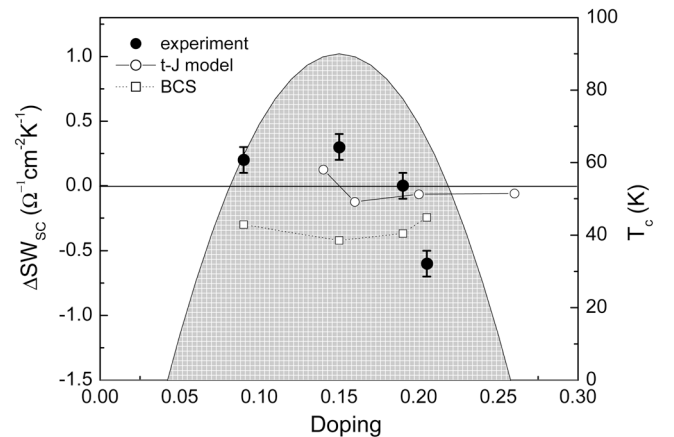


FIG. 7. Doping dependence of the superconductivity induced SW changes: experiment vs theory. Two theoretical calculations are presented: d -wave BCS model and CDMFT calculations in the framework of the t - J model.

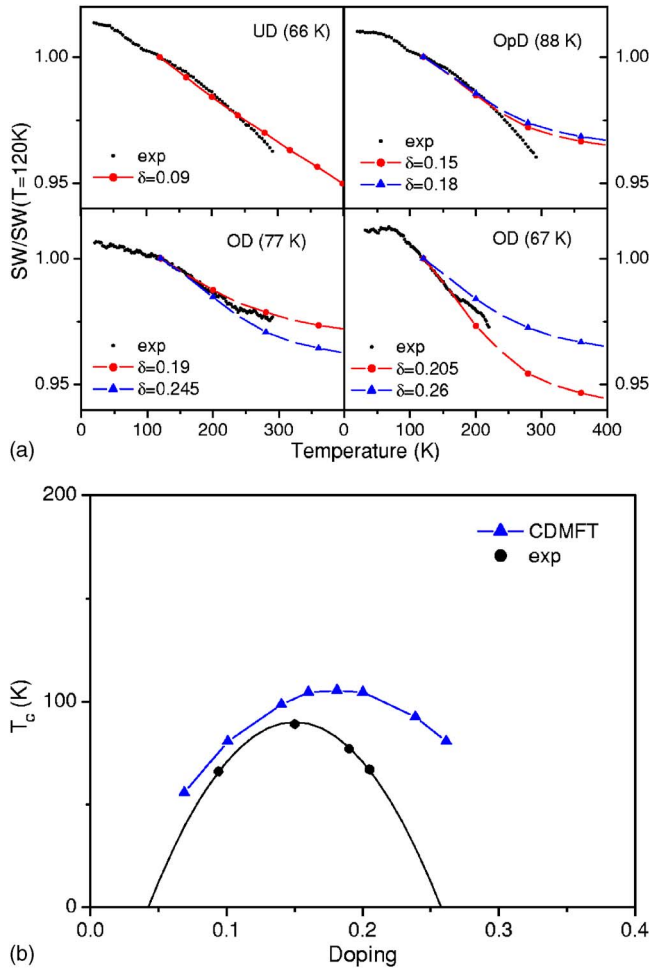


FIG. 8. (Color online) Top panel, comparison between the experimental and the theoretical $SW(T)$ in the normal state for different doping levels. Bottom panel, comparison between the dome as derived from theory and the experimental one.

result and the CDMFT calculation give $\Delta SW_{sc} > 0$ on the underdoped side of the phase diagram, and both have a change of sign as a function of doping when the doping level is increased toward the overdoped side. The data and the theory differ in the exact doping level where the sign change occurs. This discrepancy may result from the fact that for the CDMFT calculations the values $t' = t'' = 0$ were adopted. This choice makes the shape of the Fermi surface noticeably different from the experimentally known one, hence the corresponding fine-tuning of the model parameters may improve the agreement with the experimental data. This may also remedy the difference between the calculated doping dependence of T_c and the experimental one (see the right-hand panel of Fig. 8). We also show, in Fig. 9, the doping dependence of the plasma frequency and effective mass compared to the CDMFT results. One can see that a reasonable agreement is achieved for both quantities.

D. Normal state trend of the spectral weight

The persistence of the T^2 temperature dependence up to energies much larger than what usually happens in normal

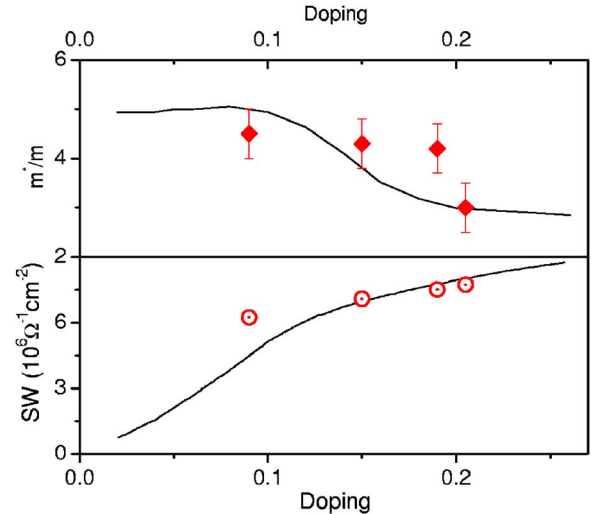


FIG. 9. (Color online) Comparison between the integrated SW and effective mass and the experimental values.

metals has been explained in the context of the Hubbard model,²⁸ showing that electron-electron correlations are most likely responsible for this effect. Indeed, experimentally we observe a strong temperature dependence of the optical constants at energies as high as 2 eV. In most of the temperature range, particularly for the samples with a lower doping level, these temperature dependencies are quadratic. Correspondingly, $SW(T)$ also manifests a quadratic temperature dependence. For sample OD67 the departure from the quadratic behavior is substantial; the overall normal state temperature dependence at this doping is also much stronger than in the other samples.

In Fig. 8 the experimental $SW(T)$ is compared to the CDMFT calculations for the same doping concentration. Since the T_c obtained by CDMFT differs from the experimental one (see Fig. 8), it might be more realistic to compare theory and experiment for doping concentrations corresponding to the same relative T_c 's. Therefore we also include in the comparison the CDMFT calculation at a higher doping level, at which $T_c/T_{c,max}$ corresponds to the experimental one (see the right-hand panel of Fig. 8). We see that the experimental and calculated values of $SW(T)$ are in quantitative agreement for the temperature range where they overlap. It is interesting in this connection that, at high temperature, the curvature in the opposite direction, clearly present in all CDMFT calculations, may actually be present in the experimental data, at least for the highly doped samples. These observations clearly call for an extension of the experimental studies to higher temperature to verify whether a crossover of the type of temperature dependence of the spectral weight really exists, and to find out the doping dependence of the crossover temperature. The experimental data, as mentioned before, show a rapid increase of the slope of the temperature dependence above optimal doping. This behavior is qualitatively reproduced by the CDMFT calculations.

IV. CONCLUSIONS

In conclusion, we have studied the doping dependence of the optical spectral weight redistribution in single crystals of

Bi2212, ranging from the underdoped regime, $T_c=66$ K to the overdoped regime, $T_c=67$ K. The low frequency SW increases when the system becomes superconducting in the underdoped region of the phase diagram, while it shows no changes in the overdoped sample $T_c=77$ K and decreases in the $T_c=67$ K sample. We compared these results with BCS calculations and CDMFT calculations based on the t - J model. We show that the latter are in good qualitative agreement with the data both in the normal and superconducting state, suggesting that the redistribution of the optical spectral weight in cuprates superconductors is ruled by electron-electron correlations effects.

ACKNOWLEDGMENTS

The authors are grateful to T. Timusk, N. Bontemps, A.F. Santander-Syro, J. Orenstein, and C. Bernhard for stimulating discussions. This work was supported by the Swiss National Science Foundation through the National Center of Competence in Research “Materials with Novel Electronic Properties—MaNEP.”

APPENDIX

The pair formation in a superconductor can be described by a spatial correlation function $g(r)$ which has a zero average in the normal state and a finite average in the superconducting state. Without entering into the details of the mechanism itself responsible for the attractive interaction between electrons, one can assume that an attractive potential $V(r)$ favors a state with enhanced correlations in the superconducting state. In the superconducting state the interaction energy differs from the normal state by

$$\langle H^i \rangle_s - \langle H^i \rangle_n = \int dr^3 g(r) V(r). \quad (\text{A1})$$

With some manipulations one can relate the correlation function to the gap function and the single particle energy. The result is a BCS equation for the order parameter, with a potential that can be chosen to favor pairing with d -wave symmetry. The simplest approach is to use a simple separable potential which leads to an order parameter of the form, Δ_k

$=\Delta_0(T)(\cos k_x - \cos k_y)/2$. The temperature dependence of $\Delta_0(T)$ can then be solved as in regular BCS theory. We have done this for a variety of parameters,¹⁴ and find that $\Delta_0(T)/\Delta_0(0) = \sqrt{1 - (t^4 + t^3)/2}$ gives a very accurate result (for either s -wave or d -wave symmetry), where $t \equiv T/T_c$. Then, for simplicity, we adopt the weak coupling result that $\Delta_0(0) = 2.1k_B T_c$. Finally, even in the normal state, the chemical potential is in principle a function of temperature (to maintain the same number density); this is computed by solving the number equation, $n = (\frac{2}{N}) \sum_k n_k$, where

$$n_k = 1/2 - (\epsilon_k - \mu) \frac{[1 - 2f(E_k)]}{2E_k},$$

where $E_k \equiv \sqrt{(\epsilon_k - \mu)^2 + \Delta_k^2}$ at each temperature for μ for a fixed doping. Once these parameters are determined, one can calculate the spectral weight sum, W , for a given band structure. We use

$$\epsilon_k = -2t * [\cos(k_x) + \cos(k_y)] + 4t' * \cos(k_x)\cos(k_y) - 2t'' * [\cos(2k_x) + \cos(2k_y)].$$

In this expression δ is the hole doping, and Δ_0 is the gap value calculated as $2.1k_B T_c$, $t=0.4$ eV, $t'=0.09$ eV and $t''=0.045$ eV. The dispersion is taken from ARPES measurements.²⁶ The spectral weight sum is given by

$$W = \sum_k \frac{\partial_k^2 \epsilon_k}{\partial k_x^2} n_k.$$

Results are plotted in Fig. 6 for the doping levels of the samples used in the experiments. These calculations clearly show that BCS theory predicts a lowering of the spectral weight sum in the superconducting phase; this is in disagreement with the experimental results in the underdoped and optimally doped samples. Moreover, there is no indication of a change of sign of the superconductivity-induced SW changes in this doping interval within the BCS formalism. Note, however, that preliminary calculations indicate that the van Hove singularity can play a role at much higher doping levels (not realized, experimentally), and that a sign change in the anomaly can occur even within BCS theory.

¹C. Proust, E. Boaknin, R. W. Hill, L. Taillefer, and A. P. Mackenzie, Phys. Rev. Lett. **89**, 147003 (2002).

²Z. M. Yusof, B. O. Wells, T. Valla, A. V. Fedorov, P. D. Johnson, Q. Li, C. Kendziora, S. Jian, and D. G. Hinks, Phys. Rev. Lett. **88**, 167006 (2002).

³A. Junod, A. Erb, and C. Renner, Physica C **317**, 333 (1999).

⁴G. Deutscher, A. F. Santander-Syro, and N. Bontemps, Phys. Rev. B **72**, 092504 (2005).

⁵R. E. Walstedt, Jr. and W. W. Warren, Science **248**, 1082 (1990).

⁶M. R. Norman, H. Ding, M. Randeria, J. C. Campuzano, T. Yokoya, T. Takeuchi, T. Takahashi, T. Mochiku, K. Kadowaki, P. Gupta, and D. G. Hinks, Nature (London) **392**, 157

(1998).

⁷A. V. Puchkov, D. N. Basov, and T. Timusk, J. Phys.: Condens. Matter **8**, 10049 (1996).

⁸H. J. A. Molegraaf, C. Presura, D. van der Marel, P. H. Kes, and M. Li, Science **295**, 2239 (2002).

⁹A. F. Santander-Syro, R. P. S. Lobo, N. Bontemps, Z. Konstantinovic, Z. Z. Li, and H. Raffy, Europhys. Lett. **62**, 568 (2003).

¹⁰A. B. Kuzmenko, H. J. A. Molegraaf, F. Carbone, and D. van der Marel, Phys. Rev. B **72**, 144503 (2005).

¹¹F. Carbone, A. B. Kuzmenko, H. J. A. Molegraaf, E. van Heumen, E. Giannini, and D. van der Marel, Phys. Rev. B **74**, 024502 (2006).

- ¹²P. F. Maldague, Phys. Rev. B **16**, 2437 (1977).
- ¹³D. van der Marel, H. J. A. Molegraaf, C. Presura, and I. Santoso, in *Concepts in Electron Correlations*, edited by A. Hewson and V. Zlatic (Kluwer, Berlin, 2003).
- ¹⁴F. Marsiglio, Phys. Rev. B **73**, 064507 (2006).
- ¹⁵H. Eskes, A. M. Oles, M. B. J. Meinders, and W. Stephan, Phys. Rev. B **50**, 17980 (1994).
- ¹⁶M. J. Rozenberg, G. Kotliar, and H. Kajueter, Phys. Rev. B **54**, 8452 (1996).
- ¹⁷P. Wrobel, R. Eder, and P. Fulde, J. Phys.: Condens. Matter **15**, 6599 (2003).
- ¹⁸Th. A. Maier, M. Jarrell, A. Macridin, and C. Slezak, Phys. Rev. Lett. **92**, 027005 (2004).
- ¹⁹K. Haule and G. Kotliar, cond-mat/0601478 (unpublished).
- ²⁰D. van der Marel, H. J. A. Molegraaf, J. Zaanen, Z. Nussinov, F. Carbone, A. Damascelli, H. Eisaki, M. Greven, P. H. Kes, and M. Li, Nature (London) **425**, 271 (2003).
- ²¹S. Tajima, G. D. Gu, S. Miyamoto, A. Odagawa, and N. Koshizuka, Phys. Rev. B **48**, 16164 (1993).
- ²²I. Bozovic, Phys. Rev. B **42**, 1969 (1990).
- ²³D. E. Aspnes, J. Opt. Soc. Am. **70**, 1275 (1980).
- ²⁴J. Wang, T. Timusk, and G. D. Dung, Nature (London) **427**, 714 (2004).
- ²⁵A. B. Kuzmenko, Rev. Sci. Instrum. **76**, 083108 (2005).
- ²⁶J. Fink, S. Borisenko, A. Kordyuk, A. Koitzsch, J. Geck, V. Zabolotnyy, M. Knupfer, B. Buechner, and H. Berger, cond-mat/0512307 (unpublished).
- ²⁷M. R. Norman and C. Pépin, Phys. Rev. B **66**, 100506(R) (2002).
- ²⁸A. Toschi, M. Capone, M. Ortolani, P. Calvani, S. Lupi, and C. Castellani, Phys. Rev. Lett. **95**, 097002 (2005).